Optoelectronic characterization of ZnS/PS systems

Caifeng Wang (王彩凤)[1*], Qingshan Li (李清山)[2], and Bo Hu (胡 波)[3]

[1]*Department of Physics and Electronics Science, Binzhou University, Binzhou 256603, China*

[2]*Physics Department, Ludong University, Yantai 264025, China*

[3]*Flying College, Binzhou University, Binzhou 256603, China*

[*]*E-mail: cfwang_2004@163.com*

Received August 11, 2008

ZnS thin films are deposited on porous silicon (PS) substrates with different porosities by pulsed laser deposition (PLD). The photoluminescence (PL) spectra of the samples are measured at room temperature. The results show that the PL intensity of PS after deposition of ZnS increases and is associated with a blue shift. With the increase of PS porosity, a green emission at about 550 nm is observed in the PL spectra of ZnS/PS systems, which may be ascribed to the defect-center luminescence of ZnS films. Junction current-voltage (I-V) characteristics were studied. The rectifying behavior of I-V characteristics indicates the formation of ZnS/PS heterojunctions, and the forward current is seen to increase when the PS porosity is increased.

OCIS codes: 250.0250, 310.6860, 230.4170.

doi: 10.3788/COL20090705.0432.

Porous silicon (PS), which is obtained by electrochemical anodization of silicon wafer in diluted HF at different current densities, is acquiring the status of a very important and versatile optoelectronic material[1]. This makes it very promising to integrate the very well-established silicon technology to optoelectronic systems[2,3]. Furthermore, the open structure and large surface area, combined with unique optical and electrical properties, make PS a good option for templates[4]. The formation of stable rectifying junctions with PS, with good forward and reverse characteristics, is one of the most challenging problems for the proper exploitation of this material in the device industry[5].

Zinc sulphide (ZnS) is a II-VI semiconductor, which has been widely investigated due to its numerous applications in n-window layers for solar cells and other optoelectronic devices[6]. Its wide band gap of about 3.7 eV makes it suitable as an ultraviolet (UV) light detector[7,8]. Crystalline ZnS has been used in electroluminescent (EL) devices such as blue or UV light emitting diodes (LEDs) and laser diodes (LDs)[9,10]. Thin films of this material have been prepared by different methods, such as chemical bath deposition, spray purolysis, and pulsed laser deposition (PLD).

In this letter, we investigate the possibility of using ZnS in conjunction with PS for fabrication of optoelectronic devices. ZnS films are prepared by PLD onto the p-type PS substrates. The photoluminescence (PL) spectroscopy is used for studying the light emission before and after the deposition. The formation of rectifying junctions is studied using current-voltage (I-V) characteristics. This method provides an easy access of the formation of heterojunctions at low temperatures.

The PS samples were formed by electrochemical anodization of (100)-oriented p-type single-crystal Si wafer with the resistivity of $7.5-11.5\ \Omega\cdot$cm. The etching was carried out in a solution of 49% HF and 99.9% ethanol ($V_{\rm HF}:V_{\rm C_2H_5OH}=1:1$) at different current densities of 5, 10, and 15 mA/cm^2 for 20 min, respectively. After anodization, the samples were rinsed in de-ionized water and dried in air. The three PS samples with different porosities were marked a, b, and c, respectively. The larger the preparation current density of PS, the greater is the porosity of the PS substrate. The thickness of porous layer was estimated to be 5 μm from the cross sectional scanning electron microscopy (SEM) measurements (not shown here). ZnS films were then deposited on the PS surface by PLD. The ZnS target (99.99%) was a sintered ceramic disc. A KrF excimer laser (Tuilaser) operating at 248 nm was used to ablate the ZnS target. Throughout the experiment, the excimer laser was set at a pulse energy of 250 mJ and a repetition rate of 2 Hz at first, then 5 Hz, so that the nanoparticles of ZnS films became integrated into the nanopores and thus the surface was effectively smoothed. The laser was focused on the target with an area of 4 mm^2, producing an energy density of 6 J/cm^2. The pulsed laser deposition chamber was first vacuumed to a base pressure of 10^{-8} Torr. The distance between the target and the substrate was 5 cm. The substrate temperature was 300 °C. The three PS samples deposited with ZnS films were correspondingly marked A, B, and C, respectively. PL studies of PS were carried out before and after the deposition of ZnS films. The excitation wavelength of 360 nm from a Xenon lamp was used. The electrical properties of the ZnS/PS samples were studied using junction I-V characteristics. A 100-nm-thick indium tin oxide (ITO) thin film was deposited also by pulsed laser on ZnS as n-type contact layer, which was carried out after ZnS films were deposited. An ohmic contact was formed by a thin Al film of about 200 nm on the back side using an electron beam evaporation (EB-500) system, which was carried out before the PS samples were prepared. The surface morphology was characterized using JSF6100 SEM. The PL spectra were measured at room temperature on RF-5301PC fluorophotometer. The electrical source of measuring I-V characteristics was provided by DH1722 direct-current (DC) voltage-stabilizing source.

The ZnS films deposited on PS were similar in nature

to that reported in our earlier publication[11]. There ZnS films were characterized by the X-ray diffraction (XRD). Figure 1 shows the SEM images of ZnS films deposited on PS substrates with different porosities. It can be seen that, when the porosity of PS substrate is small, there are some pits in the surface of ZnS films. As the substrate porosity increases, some cracks are observed which probably originate from the larger roughness of the PS surface.

All the PS samples exhibited intensive PL peaks. The intensity and the peak positions were slightly modified when ZnS films were deposited on PS. After depositing the ZnS films, the PL intensity of PS was observed to increase, with the increase of 25, 56, and 46 a.u. for samples A, B, and C, respectively, as shown in Fig. 2. It is believed that the increase in the PL peak intensity is an effect of the reduction in the nonradiative recombination centers, due to the formation of the interface between PS and nanoparticles of ZnS films[5]. In this process, the nanoparticles are expected to get embedded into the pores of PS which have similar dimensions. Figure 2(b) shows that, as the porosity of PS substrate increases, another emission band located around 550 nm in the green-light region is observed from the PL spectra of samples B and C, which is ascribed to the defect-center luminescence of ZnS[12]. The appearance of defect-center luminescence of ZnS films may be attributed to the larger roughness of the PS surface.

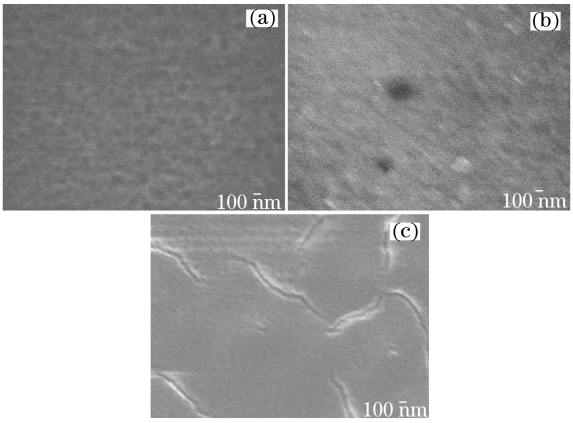

Fig. 1. SEM images of ZnS films deposited on PS substrates with different porosities. The preparation current densities of PS are (a) 5, (b) 10, and (c) 15 mA/cm^2.

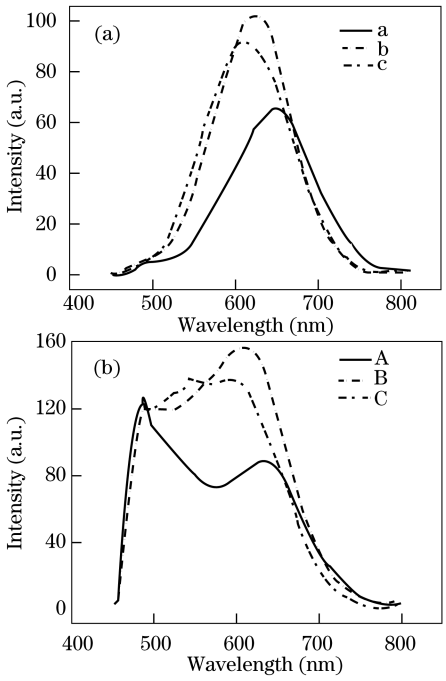

Fig. 2. PL spectra of (a) PS samples a, b, c, and (b) ZnS/PS samples A, B, and C with PS at different porosities. The preparation current densities of PS are 5, 10, and 15 mA/cm^2.

After the deposition of ZnS films, the PL peak of PS was associated with a slight blue shift. The blue shifts were 5, 17, and 23 nm for samples A, B, and C, respectively. The larger the porosity of the substrate, the greater is the blue shift of the red emission peak. It was also confirmed that the blue shift was not related to the PL emission from ZnS, but indicative of surface modification of PS after the deposition of ZnS. The PL in PS can be assumed to consist of a two-step mechanism, i.e., generation of charge carriers in the nanocrystalline silicon and recombination through the surface states. Here, the position of the recombination level, in comparison with the valence band level of PS, seems to be important in deciding whether a blue shift or a red shift is observed. The PL peak positions of PS for ZnS/PS show a blue shift as compared to that for original PS. The blue shift may be associated with the change in the energy distribution of the surface states (EDSS) in PS because the passivating bonds might be positioned much below the valence band edge of PS[13].

The I-V characteristics of the diodes consisting of ZnS/PS are shown in Fig. 3. The rectifying behavior as seen from the figure indicates the formation of heterojunctions as a result of the deposition of ZnS films. I-V characteristics show an increase in the forward current with the increase of substrate porosity. The change in the I-V characteristics for larger porosity of PS indicates the change in the forward resistance of the diode. Increase in the current density for the higher porosity of PS is expected because there would be a higher number of ZnS/PS junctions formed parallel to each other as the porosity of PS is increased.

Several other parameters are determined from the I-V characteristics. The rectification factor defined by the ratio of forward current to reverse current varies with the porosity of PS substrates, and the rectifying ratios at $\pm$7.3 V are 325, 520, and 728 at room temperature

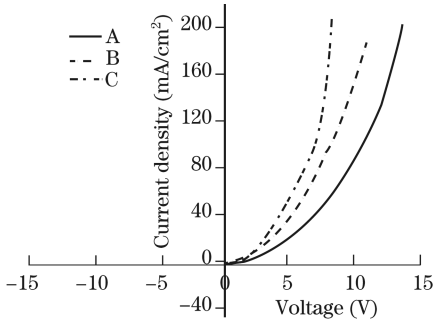

Fig. 3. I-V characteristics of ZnS/PS heterojunctions A, B, and C with PS at different porosities.

for samples A, B, and C, respectively. The onset of forward current is seen to be around +0.9 V for ZnS/PS, although there is a small variation with the porosity of PS substrates. Under reverse bias conditions, the current density is significantly low, and even zero (the error limit when measuring the current density is about ±2%). For all the diodes, the forward resistance is low (a few tens of Ω/cm^2), and the reverse resistance is considerably high. The resistance is different for different diodes. The difference can be expected because of the irregular surface of the PS and the nanocrystalline nature of the films. Another useful parameter, namely the ideality factor n, which gives the deviation of the diode characteristics from that of the ideal diode, can be calculated from the I-V plots. It is defined as[13]

$$n = \frac{q}{kT}\frac{\partial V}{\partial \ln J}, \tag{1}$$

where q is the electron charge, J is the current density, V is the applied voltage, k is the Boltzmann's constant, and T is the absolute temperature. The ideality factors for different diodes A, B, and C are calculated to be 62, 77, and 89 (T=300 K, 0 − 2 V), respectively. A large value of the ideality factor indicates a high density of trap states. High density of trap states is commonly observed in heterojunctions formed from the materials with large lattice mismatch, as PS and ZnS. Additionally, the roughness of the PS surface is also the reason for the large ideality factors.

In summary, fairly good heterostructures have been formed with ZnS films and PS substrates. High forward current density and high rectification ratio are the main features of these diodes. The junction properties of heterostructures have exhibited fairly good rectifying properties indicating that these may serve as suitable optoelectronic devices. The PL properties of ZnS/PS are very stable.

The work was supported by the Research Foundation of Young Scientists in Innovation Engineering of Binzhou University under Grant No. BZXYQNLG200703.

References

1. Y. L. Liu, Y. C. Liu, H. Yang, W. B. Wang, J. G. Ma, J. Y. Zhang, Y. M. Lu, D. Z. Shen, and X. W. Fan, J. Phys. D: Appl. Phys. **36,** 2705 (2003).
2. Y. Bai, Y. Lan, H. Zhu, and Y. Mo, Acta Opt. Sin. (in Chinese) **25,** 1712 (2005).
3. Y. Yang, Q. Li, and X. Liu, Chin. Opt. Lett. **4,** 297 (2006).
4. P. Zhang, P. S. Kim, and T. K. Sham, J. Appl. Phys. **91,** 6038 (2002).
5. A. Gokarna, S. V. Bhoraskar, N. R. Pavaskar, and S. D. Sathaye, Phys. Stat. Sol. (a) **182,** 175 (2000).
6. T. Bai, J. Ye, J. Liu, S. Wang, X. Ye, and L. Wang, Chinese J. Lasers (in Chinese) **34,** 992 (2007).
7. S. Yano, R. Schroeder, H. Sakai, and B. Ullrich, Appl. Phys. Lett. **82,** 2026 (2003).
8. S. Velumani and J. A. Ascencio, Appl. Phys. A **79,** 153 (2004).
9. T. B. Nasrallah, M. Amlouk, J. C. Bernède, and S. Belgacem, Phys. Stat. Sol. (a) **201,** 3070 (2004).
10. M. McLaughlin, H. F. Sakeek, P. Maguire, W. G. Graham, J. Molloy, T. Morrow, S. Laverty, and J. Anderson, Appl. Phys. Lett. **63,** 1865 (1993).
11. C. Wang, Q. Li, L. Lü, L. Zhang, and H. Qi, Chin. Opt. Lett. **5,** 546 (2007).
12. N. K. Morozova, I. A. Karetnikov, V. G. Plotnichenko, E. M. Gavrishchuk, É. V. Yashina, and V. B. Ikonnikov, Semiconductors **38,** 36 (2004).
13. A. Gokarna, N. R. Pavaskar, S. D. Sathaye, V. Ganesan, and S. V. Bhoraskar, J. Appl. Phys. **92,** 2118 (2002).